Integrated Technology for Detection and Repair of Mechanical Component Surface Fatigue Microcracks Using Pulsed Laser

QICHAO CHENG[1,2], DAMING ZHUANG[3], JUN HE[1,2,*] and SHIXI YANG[1,2]

-

ABSTRACT

During processing and service, various types of fatigue microcracks inevitably occur on the surfaces of mechanical components. If the microcrack is not repaired in a timely manner, it will continue to expand, affecting the safety and stability of the equipment. To this end, we introduce pulsed laser technology and propose an integrated technology for the detection and repair of mechanical component surface fatigue microcracks using pulsed laser. A finite element model is established to simulate the nonlinear interaction between fatigue microcracks and laser-generate Rayleigh wave, and the effects of parameters such as crack depth and width on the acoustic nonlinear index are investigated. On the basis of detection, the feasibility of the fatigue microcrack repair using laser melting effect is investigated. Simulation results show that contact and friction between crack interfaces must be considered, and the nonlinear modulation for Rayleigh wave mainly originates from the nonlinear interaction between the longitudinal wave component and the fatigue microcrack. The acoustic nonlinear index of longitudinal wave increases and decreases with the increase of crack depth and width, respectively. In addition, fatigue crack repair is feasible by properly adjusting laser parameters.

INTRODUCTION

Mechanical components inevitably generate fatigue microcracks due to the effects of stress and the environment. If early fatigue microcracks are not detected and repaired in a timely manner, they will continue to propagate until failure occurs, resulting in serious accidents and significant economic losses. In addition, according to relevant statistics [1], early fatigue damage accounts for approximately 80-90% of the entire lifespan of mechanical components. Therefore, it is of great importance to employ appropriate non-destructive testing methods to detect early fatigue microcracks in a timely manner [2]. Traditional ultrasonic testing methods primarily rely on the interaction of ultrasonic waves with defects, including reflection, transmission, and

[1]State Key Laboratory of Fluid Power Components and Mechatronic Systems, Zhejiang University, Hangzhou, China
[2]School of Mechanical Engineering, Zhejiang University, Hangzhou, China
[3]Hangzhou Steam Turbine Power Group Co.,Ltd., Hangzhou, China

Corresponding author:
Jun He, School of Mechanical Engineering, Zhejiang University, No. 866 Yuhangtang Road, Xihu District, Hangzhou, 310058, China.
Email: hjshenhua@zju.edu.cn

scattering, to detect and evaluate macroscopic defects in materials [3]. However, they are not sensitive enough to detect early fatigue cracks at the micro-nanoscale. Nonlinear ultrasonic can overcome the limitations of traditional linear ultrasonic testing methods and effectively identify fatigue microcracks based on the nonlinear modulation effect between ultrasonic waves and microcracks [4].

According to the frequency difference of the excited ultrasonic waves, the nonlinear ultrasonic detection methods can be divided into single-frequency detection [5], mixed-frequency detection [6], and broadband detection [7]. Nonlinear laser ultrasonic is a new non-contact non-destructive testing method that has been developed based on traditional contact-based nonlinear ultrasonic. It utilizes the specimen itself as a transducer and has characteristics such as non-contact, wide frequency range, multi-mode, and high spatial resolution [8]. The interaction between laser-excited broadband ultrasonic waves and fatigue microcracks results in nonlinear modulation on the input frequency components. This leads to a highly complex and chaotic frequency spectrum, making it difficult to extract nonlinear features [9]. There are two common methods to address this issue. The first is to employ advanced signal processing methods to analyze the sidebands of the nonlinear ultrasonic signals and extract nonlinear features related to fatigue crack size. Liu et al. [10] extracted the Bhattacharyya Distance (BD) in the state space of nonlinear laser ultrasonic signals as a nonlinear feature to evaluate fatigue damage. The second is to modify the pulse laser excitation way to narrow down the frequency range of the generated ultrasonic waves. Kou et al. [11] transformed the laser point source into a laser grating source to excite narrowband surface acoustic waves at specific frequencies and utilized the nonlinear modulation of the acoustic surface waves to detect closed surface cracks.

Repairing for fatigue microcracks after detection is of great significance in extending the lifespan of mechanical components, and laser repair has become one of the most important methods due to its high efficiency and high precision characteristics. Currently, commonly used laser repair methods mainly include laser additive manufacturing [12], laser cladding [13], and laser melting [14], in which laser melting is widely used due to its simplicity and high repair efficiency. The principle of laser melting is to use a high power density laser to melt or even vaporize a localized area of the material surface in an instant, followed by rapid solidification. The microstructure of the surface layer after solidification is tiny, with high hardness and good fatigue resistance.

A large number of scholars have done a great deal of work on detection and repair for fatigue microcracks, yet few scholars have integrated them at present. For this reason, we introduced laser technology and proposed an integrated technology for detection and repair of surface fatigue microcracks using pulsed laser. The technical route is shown in Figure 1, and this integrated technique can improves the detection accuracy and repair efficiency. In this article, we first give the technical route of the integrated technology for detection and repair. Then a finite element model is established to simulate the nonlinear interaction between fatigue microcracks and laser-generate Rayleigh wave, and the effects of parameters such as crack depth and width on the acoustic nonlinear index are investigated. Finally, the feasibility of laser melting repair for fatigue microcracks is investigated on the basis of detection.

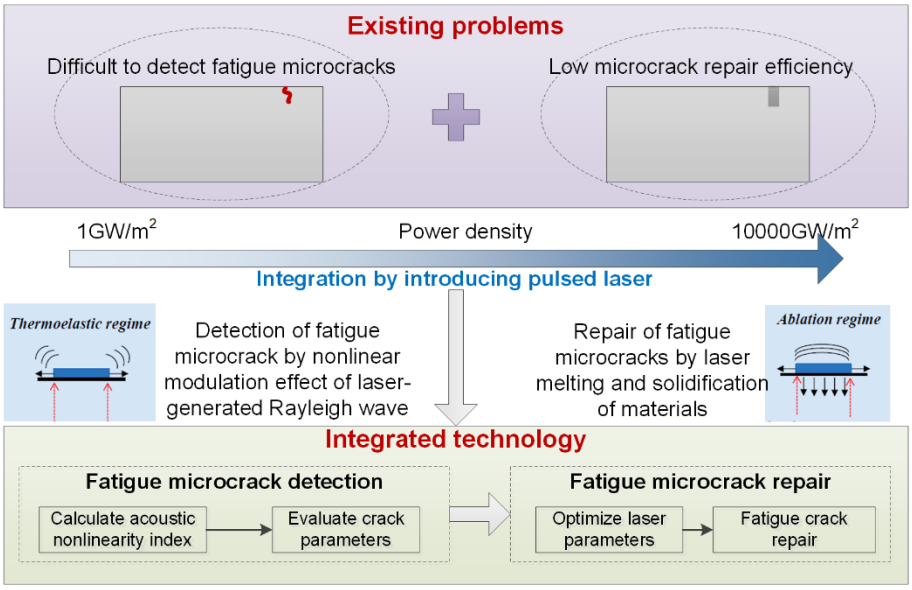

Figure 1. Technical route for the integration of detection and repair

THEORETICAL BASIS

In the thermoelastic regime, the material absorbs electromagnetic irradiation from the laser to form an inhomogeneous temperature field:

$$\rho c\dot{T}(x,y,t) = k\nabla^2 T(x,y,t) \tag{1}$$

Where $T(x,y,t)$ is the time-dependent temperature field varying along the length direction x and depth direction y. ρ, c, and k represent the density, specific heat capacity and thermal conductivity, respectively.

The temperature gradient in the temperature field induces thermal expansion, leading to the generation of the Rayleigh wave propagating along the specimen surface and the bulk wave propagating inside the specimen.

$$(\lambda+\mu)\nabla(\nabla\bullet U(x,y,t)) + \mu\nabla^2 U(x,y,t) = \rho\ddot{U}(x,y,t) + (3\lambda+2\mu)\alpha\nabla T(x,y,t) \tag{2}$$

Where $U(x,y,t)$ is the time-dependent displacement field varying along the length direction x and depth direction y. λ and μ are the Lame constants, and α is the coefficient of thermal expansion.

Under the action of laser-generated Rayleigh wave, contact and friction between crack interfaces occur, resulting in contact nonlinearity. The contact force between crack interfaces can be calculated using the nonlinear spring model and the frictional force between crack interfaces can be calculated using Coulomb law.

In the ablation regime, the laser power density exceeds the threshold and the specimen surface undergoes melting, vaporization, and plasma. According to the heat flux absorbed by the material gasification, the ablation velocity for the material at the boundary can be calculated:

$$v_a = h_a(T_a - T)/(\rho H_s) \quad (3)$$

Where h_a denotes temperature-dependent heat transfer coefficient, T_a denotes ablation temperature, H_s denotes sublimation heat.

SIMULATION MODEL

As shown in Figure 2, a 2D finite element simulation model is established to investigate the nonlinear interaction between the Rayleigh wave and the fatigue microcrack in an aluminum block by COMSOL Multiphysics 5.6 software. The model size is 16mm*5mm. The laser excitation point is located in the center of the upper surface, and the surface fatigue microcrack and detection point are 5mm and 6 mm away from the laser excitation point, respectively. The width and depth range of cracks are 10-100nm and 0.6-1.0mm, respectively, and contact and friction are set between the crack interfaces. In addition, the laser spot radius, rise time, and maximum laser power density are 300μm, 10ns and 1.8*10^{11}W/m2, respectively. Considering computational accuracy and efficiency, the maximum mesh size and time step are set 50μm and 10ns, respectively.

SIMULATION RESULTS AND DISCUSSION

The ultrasonic field generated after laser irradiation is shown in Figure 3(a), the Rayleigh wave that is elliptically polarized and propagates in the x-direction can be viewed as a synthesis of shear and longitudinal waves. Therefore, the displacement components of the Rayleigh wave in the x and y directions represent the longitudinal and shear waves, respectively, as shown in Figure 3(b) and (c). In order to accurately reveal the nonlinear modulation effect of fatigue microcracks on Rayleigh waves, the interaction between the fatigue microcrack and the longitudinal and shear components of the Rayleigh wave are investigated separately. The longitudinal and shear wave received at the detection point with and without the fatigue microcrack are presented in Figure 3(d) and (e). When the fatigue microcrack occurs, the signal amplitude decreases significantly in both the longitudinal and shear components, and the waveforms of the shear wave component remain essentially unchanged, while the waveforms of the longitudinal wave component change significantly.

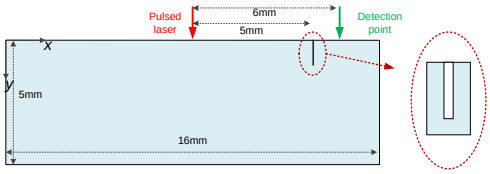

Figure 2. Schematic diagram of finite element model.

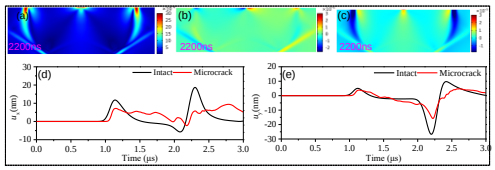

Figure 3. (a) Ultrasonic field and its (b) *x*-component and (c) *y*-components at 2200ns, (d) the *x*-component (longitudinal wave) and (e) *y*-component (shear wave) of the received Rayleigh wave at a surface detection point located 6mm away from the laser source with and without a fatigue microcrack

Complex interactions between the longitudinal and shear waves and the fatigue microcrack lead to changes in their waveforms. As shown in Figure 4(a), the variation trend of the longitudinal wave is mainly divided into three stages, and in the first stage, the head wave and the stretching phase of the longitudinal wave plays a major role. In Figure 4(c), at 1050ns, the head wave directly propagates through the crack interface after encountering a microcrack, and there is an uneven distribution of contact pressure at the crack interface. At 1700ns, the stretching phase of the longitudinal wave meets the microcrack and pulls the closed crack apart into an open crack, at this time, the longitudinal wave can only propagate through the crack contour, and there is no contact pressure at the crack interface. The second stage is mainly dominated by the compression phase of the longitudinal wave. At 1950ns, the compressional phase of the longitudinal wave squeezes the crack interface to make contact so that the longitudinal wave can propagate, and at this time, there is also an uneven contact pressure. The third stage is mainly due to the scattering of the longitudinal wave. At 2600 ns, a portion of the longitudinal wave with a wavelength exceeding the length of the defect front edge continues to propagate along the crack contour, undergoing reflection, transmission and scattering until it reaches the detection point, at which time there is also no contact pressure. Similar to the longitudinal wave, the waveform change of the shear wave is also divided into three phases, and the friction pressure is accompanied by the contact pressure, which affects its waveform.

A key feature of closed cracks compared to open cracks is the ability to contact and friction between crack interfaces, the effect of which on the results is shown in Figure 5. It can be seen from Figure 5(a) and (c) that when contact and friction are not considered, the transmitted longitudinal and shear waves have a smooth bipolar waveform. When contact is considered, the transmitted longitudinal wave increases multiple peaks and the waveform of the transmitted shear wave becomes narrower. It can be noticed from the wavefield snapshots in Figure 5(b) and (d) that there is a portion of longitudinal and shear waves directly transmitted through the crack interface thus changing the waveform. When friction is further considered on top of contact, the transmitted longitudinal wave gains several peaks and the amplitude of the transmitted transverse wave increases, it can be found from the wavefield snapshots that the friction and slip generated by the contact affects the wave propagation. This can be explained by the three mechanisms in Figure 5(e). When there is no contact or friction, longitudinal and shear waves mainly propagate to the detection point through the crack contour. When considering contact, longitudinal and shear waves can be directly transmitted to the detection point through the crack interface. After further consideration of friction, the propagation of longitudinal and shear waves along the crack interface will be affected by slip effects

In Figure 6(a), as the depth increases, the peak amplitude of the longitudinal wave increases at 2.05μs and decreases at 2.5μs. This is because the contact area between cracks increases with depth, resulting in an increase in the longitudinal wave propagation directly through the crack interface, while the front and rear edges of the crack increase, and the longitudinal wave propagating along the crack contour decreases. In Figure 6(c), the peak amplitude of the shear wave at 2.2μs increases with increasing depth, which is also due to the reduction of the propagating shear wave along the crack profile. It can be observed from Figure 6 (b) and (d) that obvious second harmonics appear in the frequency spectrum of the longitudinal wave, reflecting the contact nonlinearity, while in the frequency spectrum of the shear wave the second harmonics

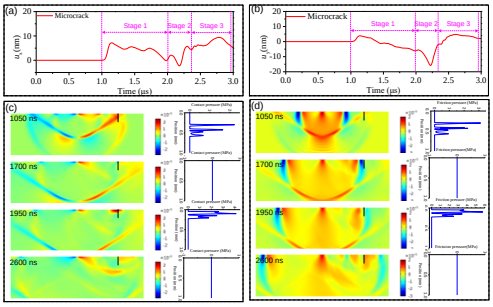

Figure 4. The interaction between laser-generated Rayleigh wave and a fatigue microcrack. The waveform of (a) longitudinal wave and (b) shear wave with a fatigue microcrack, (c) the longitudinal wavefield and corresponding contact pressure at different time, (d) the shear wavefield and corresponding friction pressure at different time.

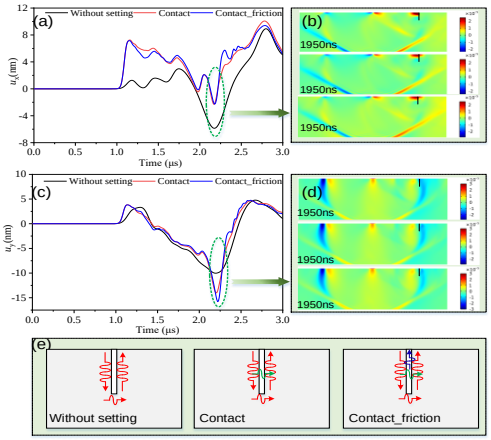

Figure 5. (a) The waveform and (b) wavefield for longitudinal wave and (c) the waveform and (d) wavefield for shear wave under three conditions, (e) the mechanisms of nonlinear interaction between the Rayleigh wave and the fatigue microcrack under three conditions.

are not obvious, only the frequency band of the signal decreases, reflecting the low-pass filtering properties of the cracks. As shown in Figure 6(e), the fundamental amplitude of the longitudinal wave decreases with increasing crack depth, while the second harmonic amplitude first decreases and then increases. Further, an acoustic nonlinearity index $\beta = A_2 / (A_1^2)$ (A_1 is the fundamental amplitude, A_2 is the second harmonic amplitude) is introduced to characterize the crack extension, and it is observed that the acoustic nonlinearity index increases monotonically with the increase of crack depth. Therefore, the crack depth can be effectively identified by the established mapping relationship between the acoustic nonlinearity index and the crack width.

In Figure 7, when the crack width increases to 60nm, the longitudinal waveform no longer shows any change, indicating that the limiting width at which contact nonlinearity can occur is 50nm. In the wavefield snapshots, when the crack width is larger than 50 nm, basically no longitudinal wave can directly transmit through the crack interfaces.

Further research is conducted on the influence of crack width within 50nm on ultrasonic waveform and acoustic nonlinearity index. In Figure 8(a) and (c), as the width increases, the amplitude of the longitudinal wave decreases gradually in the range of 2.0 μ s-2.5μs and remains essentially unchanged at 2.8μs, and the amplitude of the shear wave decreases at 2.2μs. In Figure 8(b) and (d), there is a significant second harmonic in the frequency spectrum of the longitudinal wave, while in the frequency spectrum of shear wave, the second harmonic is not significant, only the entire frequency band decreases. In Figure 8(e), as the crack width increases, the acoustic nonlinearity index monotonically decreases. Therefore, the established mapping relationship between the acoustic nonlinearity index and the crack width can effectively identify the crack width.

Fatigue microcracks need to be repaired in a timely manner after identification, and they are usually buried at small depths and can be repaired efficiently using pulsed laser melting method. In this paper, only a brief discussion of laser melting repair for fatigue microcracks is presented. Parameters such as laser energy, pulse width, and spot

diameter all affect ablation depth and melting depth, with laser energy being the most important parameter available for adjustment. The temperature field at different laser energies is shown in Figure 9, when the laser power density is that used for the previous thermoelastic excitation, the maximum temperature has not yet reached the melting point of aluminum (660℃). When the laser power density increases by 10 times, the maximum temperature exceeds the gasification temperature of aluminum (2500℃). When the laser power density increases by 100 times, the maximum temperature reaches 35400℃, and the ablation depth increases. Therefore, after determining the depth of the fatigue microcrack, the appropriate laser power density and repetition frequency can be selected to ablate the fatigue microcrack to repair the surface.

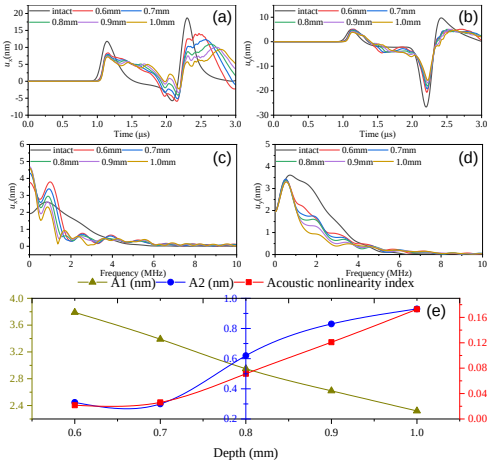

Figure 6. (a) The waveform of the longitudinal wave and (b) corresponding frequency spectrum, as well as (c) the waveform of the shear wave and (d) corresponding frequency spectrum under different crack depths, (e) the relationship between the acoustic nonlinearity index with crack depth.

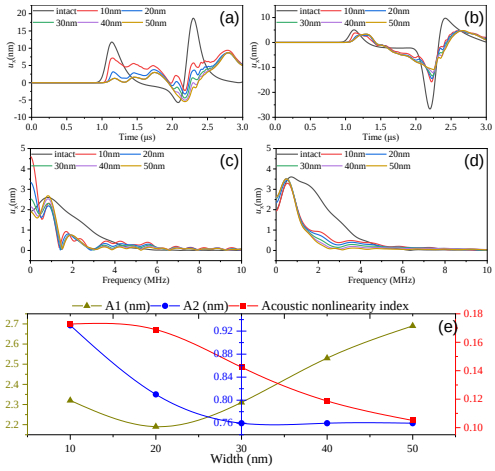

Figure 8. (a) The waveform of the longitudinal wave and (b) corresponding frequency spectrum, as well as (c) the waveform of the shear wave and (d) corresponding frequency spectrum under different crack widths, (e) the relationship between the acoustic nonlinearity index with crack widt

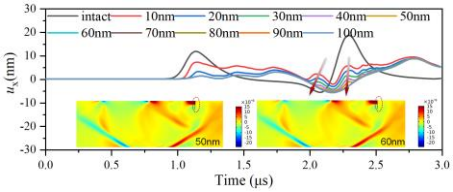

Figure 7. The transition of wavefield and waveform for longitudinal wave at the critical width.

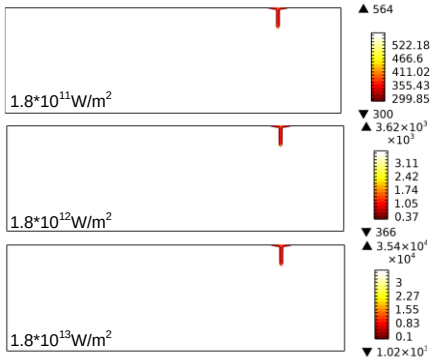

Figure 9. The temperature field at different laser energies.

CONCLUSIONS

In this paper, we propose an integrated technology for the detection and repair of mechanical component surface fatigue microcracks using pulsed laser. A finite element model is established to simulate the nonlinear modulation effect of the fatigue microcracks on the Rayleigh wave and the feasibility of fatigue crack repair using laser melting is investigated. Some conclusions obtained are as follows: (1) The Rayleigh wave consist of the longitudinal and shear waves, and their nonlinear modulation mainly originates from the nonlinear interaction between the longitudinal wave component and the fatigue microcrack. (2) Contact and friction between crack interfaces have a significant effect on the waveform and must be considered in the calculations. (3) The acoustic nonlinear index of longitudinal wave increases and decreases with the increase of crack depth and width, respectively. (4) By increasing laser energy, surface areas with fatigue microcracks can be melted and ablated to extend service life.

REFERENCES

1. Meyendorf, N. G. H., Rosner, H., Kramb, V., and Sathish S. 2002. "Thermo-acoustic fatigue characterization," Ultrasonics, 40(1-8): 427-434.
2. Sagar, S. P., Das, S., Parida, N., and Bhattacharya, D. K. 2006. "Non-linear ultrasonic technique to assess fatigue damage in structural steel," Scr. Mater., 55(2): 199-202.
3. He, J., Liu, X. K., Cheng, Q. C., Yang, S. X., and Li, M. S. 2023. "Quantitative detection of surface defect using laser-generated Rayleigh wave with broadband local wavenumber estimation," Ultrasonics, 132(9): 106983.
4. Sampath, S., and Sohn, H. 2022. "Detection and localization of fatigue crack using nonlinear ultrasonic three-wave mixing technique," Int. J. Fatigue, 155(11): 106582.
5. Lyu, W. H., Wu, X. M. and Xu, W. J. 2019. "Nonlinear Acoustic Modeling and Measurements during the Fatigue Process in Metals," Materials, 12(4): 12040607.
6. Korneev, V. A. and Demcenko, A. 2014. "Possible second-order nonlinear interactions of plane waves in an elastic solid," J. Acoust. Soc. Am., 135(2): 591-598.
7. Wang, Q. Y., Xu, Y., and Liu, C. Y. 2022. "Concrete Microcracks Detection under Compressive Load Based on Nonlinear Ultrasonics Modulation with Broadband Excitation," Res. Nondestruct. Eval., 33(2): 98-120.
8. Liu, P., Yi, K., Park, Y., and Sohn, H. 2022. "Ultrafast nonlinear ultrasonic measurement using femtosecond laser and modified lock-in detection," Opt. Lasers Eng., 150(11): 106844.
9. Liu, P., Sohn, H., and Park, B. 2015. "Baseline-free damage visualization using noncontact laser nonlinear ultrasonics and state space geometrical changes," Smart Mater. Struct., 24(6): 065036.
10. Liu, P. P., Nazirah, A. W. and Sohn, H. 2016. "Numerical simulation of damage detection using laser-generated ultrasound," Ultrasonics, 69: 248-258.
11. Kou, X., Pei, C. X., and Chen, Z. M. 2021. "Fully noncontact inspection of closed surface crack with nonlinear laser ultrasonic testing method," Ultrasonics, 114: 106426.
12. Molina, C., Araujo, A., Bell, K., Mendez, P. F., and Chapetti, M. 2021. "Fatigue life of laser additive manufacturing repaired steel component," Eng. Fract. Mech., 241: 107417.
13. Gardner, P. F., Noone, S. J., Bandyopadhyay, R., Park, J. S., Walker, K., and Sangid, M. D. 2022. "Damage Tolerance Assessment of Laser Clad Repairs of Coarse Grain Ti-6Al-4V," Exp. Mech., 62(8): 1421-1436.
14. Ma, S. Y., Zhou, T., Zhou, H., Chang, G., Zhi, B. F., and Wang, S. Y. 2020. "Bionic Repair of Thermal Fatigue Cracks in Ductile Iron by Laser Melting with Different Laser Parameters," Metals, 10(1): 10010101.